

Ferroelectric and Antiferroelectric Behavior in Chiral Bent-shaped Molecules with an Asymmetric Central Naphthalene Core

Seng Kue Lee,* Masatoshi Tokita, Yoshio Shimbo, Kyung-Tae Kang,† Hideo Takezoe, and Junji Watanabe

Department of Organic and Polymeric Materials, Tokyo Institute of Technology, Tokyo 152-8552, Japan

*E-mail: sklee@polymer.titech.ac.jp

†Department of Chemistry and Chemistry Institute for Functional Materials, Pusan National University, Busan 609-735, Korea

Received March 8, 2007

A new series of chiral bent-shaped liquid crystals with an asymmetric central core based on 1,6-dihydroxynaphthalene and chiral terminal chain prepared from (*S*)-(-)-2-methyl-1-butanol, 1,6-naphthalene bis[4-(4-alkoxyphenyliminomethyl)]benzoates [N(1,6)-*n*-O-PIMB(*n*-2)*-(*n*-4)O (*n* = 8-11)] were synthesized. Their mesomorphic properties and phase structures were investigated by means of electro-optical, polarization reversal current, and second harmonic generation measurements in order to confirm the relationship between the molecular structure and phase structure. All odd *n* (*n* = 9 and 11) compounds, N(1,6)-9-O-PIMB7*-5O and N(1,6)-11-O-PIMB9*-7O exhibit antiferroelectric phase, whereas even *n* (*n* = 8 and 10) compounds was flexible, N(1,6)-10-O-PIMB8*-6O exhibits the ferroelectric phase but N(1,6)-8-O-PIMB6*-4O exhibits the antiferroelectric phase. These results come from the decrease of the closed packing efficiency within a layer and the lack of uniform interlayer interaction between adjacent layers, which were caused by the asymmetrical naphthalene central core. Thus, we concluded that the structure of central core as well as the terminal chain plays an important role for the emergence of particular polar ordering in phase structures.

Key Words : Bent-shaped liquid crystals, Ferroelectricity and antiferroelectricity, Odd-even behavior, 1,6-Dihydroxynaphthalene, (*S*)-(-)-2-Methyl-1-butanol

Introduction

Ferroelectric¹ and antiferroelectric² properties in liquid crystals were usually found in the chiral molecular systems. Until recently, chirality was considered to be necessary to produce polar order in each layer, since the removed symmetry of mirror planes is responsible for the genesis of ferroelectric and antiferroelectric ordering. However, Niori *et al.*³ discovered that achiral bent-shaped molecules (so called banana molecules) can also form polar smectic layers and exhibit ferroelectric and antiferroelectric behavior with electro-optic switching although the molecules themselves are not chiral. Since this discovery, a number of achiral bent-shaped molecules have been reported⁴⁻⁸ and bent-shaped molecules with chiral terminal groups have also been studied extensively in order to investigate the relationship between the terminal chain and phase structure.⁹⁻¹² One of the most widely investigated bent-shaped mesophase is the B2 phase because of its polar switching.³ In the B2 phase, the molecules are tilted from the layer normal, resulting in unique layer chirality.¹³ Depending on tilt and polar correlation between adjacent layers four phase structures differing in chirality and polarity are formed.¹³ These are distinguished using the nomenclature SmC_{S,A}P_{F,A}. Here, the first two subscripts, S and A, specify synclincity and anticlincity, and second two subscripts, F and A, specify ferroelectricity and antiferroelectricity, respectively. Moreover, in accordance with the switching current measurement of these molecules most of them exhibit the antiferroelectric mesophase in the ground state although a few ferroelectric

bent-shaped mesogens have been found.¹⁴⁻²⁴

Recently, Kumazawa *et al.*²⁵ and Lee *et al.*²⁶ reported an odd-even behavior on the emergence of ferroelectricity and antiferroelectricity in two homologous series of bent-shaped mesogens with chiral terminal chains, P*n*-O-PIMB(*n*-2)* (*n* = 6-10) and their oxygen analogues P*n*-O-PIMB(*n*-2)*-(*n*-4)O (*n* = 8-10), in which one methylene unit is replaced by an oxygen atom and found that the interlayer steric interaction plays a major role for the emergence of a variety of phase structures, and especially the directions of methyl groups connected to the chiral centers in these compounds play a key role in determining ferroelectricity and antiferroelectricity. In addition Nishida *et al.*²⁷ showed that this role was valid even in mixtures of two bent-shaped mesogens with different terminal chain lengths and in bent-shaped mesogens with nonsymmetrical terminal chains. Namely, a longer chain always governs the odd-even rule. However, the central core ring in these molecules were composed of symmetrical resorcinol derivatives substituted at the 1,3-position in benzene ring and it might be a important factor on the phase structure because the closed packing of central cores makes the position of end of terminal chains fixed. More recently, Lee *et al.*²⁸ described the mesomorphic properties of six bent-shaped molecules with side wings at different positions of central naphthalene ring containing a Schiff's based moiety. Among those, N(1,6) composing of naphthalene derivatives substituted at the 1,6-position showed the most typical B2 phase and exhibited an antiferroelectric response in switching behavior by applying an electric field.

In this report, we describe the synthesis of new bent-shaped molecules N(1,6)-*n*-O-PIMB(*n*-2)*-(*n*-4)O (*n*=8-11) with an asymmetric central core based on 1,6-dihydroxynaphthalene and chiral terminal chain prepared from (*S*)-(-)-2-methyl-1-butanol. We also demonstrate their phase structures and mesomorphic properties by means of electro-optical, polarization reversal current, and second harmonic generation (SHG) measurements in order to confirm the effect of the asymmetric central core and terminal chains on the phase structure.

Experimental

Measurements. All used reagents were purchased from TCI (Tokyo Kasei Kogyo Co., LTD.) and used without further purification. Solvents were purified by normal procedures and handled under a moisture free atmosphere. Column chromatography was performed using silica gel (Merck, 230-400 mesh). ¹H NMR spectra were recorded on JEOL FT-NMR AL 400 (400 MHz) spectrometers using chloroform as an internal standard. Elemental analysis was determined by CHNS-932 & VTF-900. The texture observation was made under crossed polarizers using Olympus BX50 polarizing optical microscopy (POM) equipped with a temperature controlled Mettler Toledo FP 82 hot stage. Transition temperatures were determined by differential scanning calorimetry (DSC) using a Perkin-Elmer DSC 7 calorimeter. Electro-optic switching behavior was observed using a high speed voltage amplifier (FLC Electronics, F20A) connected to a function generator (NF Electronic Instruments, WF 1945A). The sample was sandwiched between glass substrates with ITO electrodes and the thickness was 5.3-9.2 μm. The polarization reversal current was measured by applying a triangular wave voltage. SHG intensity was observed by the oblique incidence (45°) of a p-polarized fundamental wave from a Nd:YAG laser (Quanta-Ray, DCR-11) to the cell. Signals were detected with a photomultiplier tube (Hamamatsu R-955) after passing through appropriate optical filters, and output signals were

accumulated by a BOXCAR system (Stanford Research Systems).

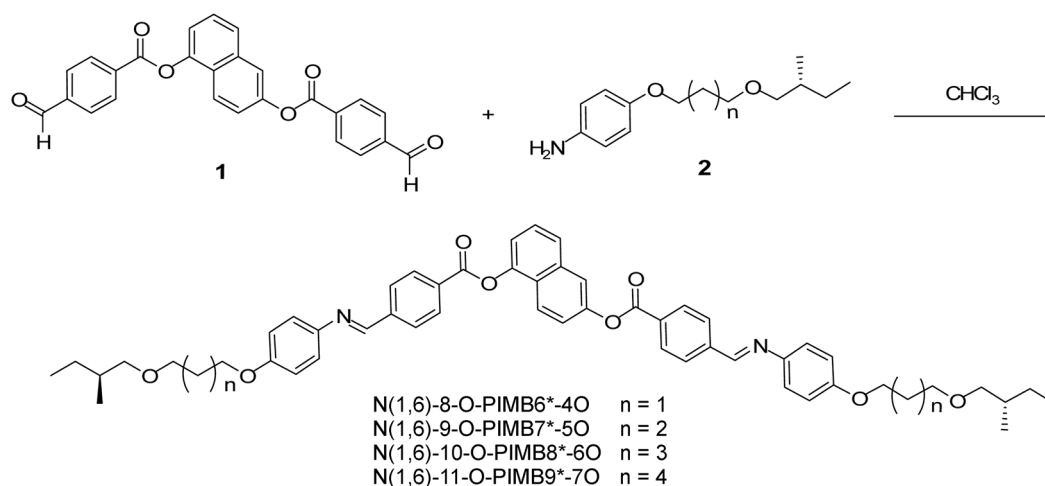
Synthesis. The synthetic route to the target compounds is illustrated in Scheme 1. The preparation of the naphthalene-1,6-diyl bis(4-formylbenzoate) **1** and 4-[(*S*)-6-methyl-4-oxa-1-octyl] aniline **2** were performed using procedures described in our previous report.^{26,28}

1,6-Naphthalene bis[4-(4-alkoxyphenyliminomethyl)]-benzoates: A solution of **2** (0.3 g, 1.26 mmol) and bis-aldehyde **1** (0.24 g, 0.57 mmol) in chloroform (20 mL) was heated under flux for 3 h. The reaction mixture was concentrated and recrystallized from chloroform/ethanol to give 0.39 g (80%) of N(1,6)-8-O-PIMB6*-4O as yellow crystals. Final compounds N(1,6)-*n*-O-PIMB(*n*-2)*-(*n*-4)O (*n* = 9-11) were similarly prepared in 85%, 83%, and 85% yield, respectively.

For N(1,6)-8-O-PIMB6*-4O, ¹H-NMR (400 MHz, CDCl₃) δ 0.87-0.90 (m, 12H), 1.07-1.69 (m, 6H), 2.07 (quin, *J* = 6.0 Hz, 2H), 2.08 (quin, *J* = 6.0 Hz, 2H), 3.19-3.30 (m, 4H), 3.60 (t, *J* = 6.0 Hz, 4H), 4.11 (t, *J* = 6.0 Hz, 2H), 4.12 (t, *J* = 6.0 Hz, 2H), 6.95-8.10 (m, 18H), 8.33 (d, *J* = 8.4 Hz, 2H), 8.42 (d, *J* = 8.4 Hz, 2H), 8.59 (s, 1H), 8.62 (s, 1H). Anal. Calc. for C₅₄H₅₈N₂O₈: C 75.15, H 6.77, N 3.25, O 14.83; found: C 74.12, H 6.77, N 3.07, O 15.45.

For N(1,6)-9-O-PIMB7*-5O, ¹H-NMR δ 0.88-0.92 (m, 12H), 1.08-1.69 (m, 6H), 1.77 (quin, *J* = 6.0 Hz, 4H), 1.90 (quin, *J* = 6.0 Hz, 4H), 3.18-3.31 (m, 4H), 3.48 (t, *J* = 6.0 Hz, 4H), 4.03 (t, *J* = 6.0 Hz, 2H), 4.04 (t, *J* = 6.0 Hz, 2H), 6.94-8.10 (m, 18H), 8.33 (d, *J* = 8.4 Hz, 2H), 8.42 (d, *J* = 8.4 Hz, 2H), 8.59 (s, 1H), 8.62 (s, 1H). Anal. Calc. for C₅₆H₆₂N₂O₈: C 75.48, H 7.01, N 3.14, O 14.36; found: C 73.93, H 6.96, N 2.95, O 14.15.

For N(1,6)-10-O-PIMB8*-6O, ¹H-NMR δ 0.88-0.91 (m, 12H), 1.07-1.87 (m, 18H), 3.16-3.29 (m, 4H), 3.43 (t, *J* = 6.0 Hz, 4H), 4.06 (t, *J* = 6.0 Hz, 2H), 4.07 (t, *J* = 6.0 Hz, 2H), 6.93-8.10 (m, 18H), 8.33 (d, *J* = 8.4 Hz, 2H), 8.42 (d, *J* = 8.4 Hz, 2H), 8.58 (s, 1H), 8.61 (s, 1H). Anal. Calc. for C₅₈H₆₆N₂O₈: C 75.79, H 7.25, N 3.05, O 13.93; found: C 75.06, H 7.15, N 2.93, O 14.30.



Scheme 1

Table 1. Transition temperatures (°C) for the N(1,6)-*n*-O-PIMB-(*n*-2)*-(*n*-4)O series on cooling at a rate of 10 °C min⁻¹

Compound	Crystal	B2	Iso	mp
N(1,6)-8-O-PIMB6*-4O	104.9	145.5	120.6	
N(1,6)-9-O-PIMB7*-5O	101.5	166.3	123.0	
N(1,6)-10-O-PIMB8*-6O	85.8	162.1	107.5	
N(1,6)-11-O-PIMB9*-7O	76.9	159.3	106.9	

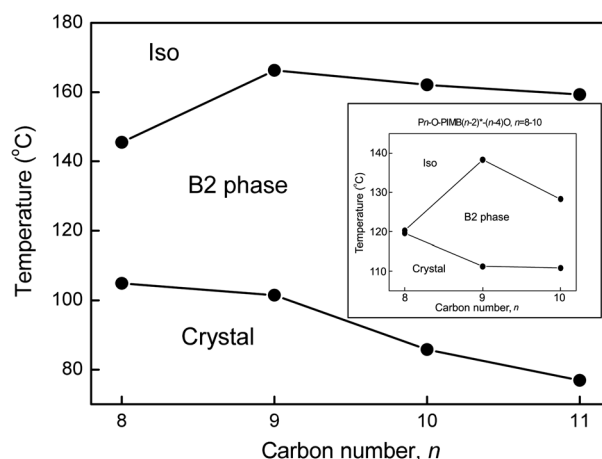
For N(1,6)-11-O-PIMB9*-7O, ¹H-NMR δ 0.87-0.91 (m, 12H), 1.06-1.85 (m, 22H), 3.15-3.29 (m, 4H), 3.41 (t, *J* = 6.0 Hz, 4H), 4.00 (t, *J* = 6.0 Hz, 2H), 4.01 (t, *J* = 6.0 Hz, 2H), 6.94-8.10 (m, 18H), 8.33 (d, *J* = 8.4 Hz, 2H), 8.42 (d, *J* = 8.4 Hz, 2H), 8.60 (s, 1H), 8.62 (s, 1H). Anal. Calc. for C₆₀H₇₀N₂O₈: C 76.08, H 7.45, N 2.96, O 13.51; found: C 76.13, H 7.31, N 2.87, O 13.66.

Results

New chiral bent-shaped liquid crystals with an asymmetric central core based on 1,6-dihydroxynaphthalene, N(1,6)-*n*-O-PIMB(*n*-2)*-(*n*-4)O (*n* = 8-11) were synthesized and their physical properties were investigated by electric and optical measurements. Table 1 summarized the mesomorphic transition temperatures collected from DSC in conjunction with POM. All compounds enantiotropically exhibit the typical B2 phase on cooling from the isotropic liquid phase, and crystallization temperatures decrease as the chain length of the terminal alkyl increases. Especially, the compound N(1,6)-11-O-PIMB9*-7O exhibited the lowest crystallization temperatures (76.9 °C) and also the broadest temperature range (82.4 °C) of the B2 phase among the prepared compounds.

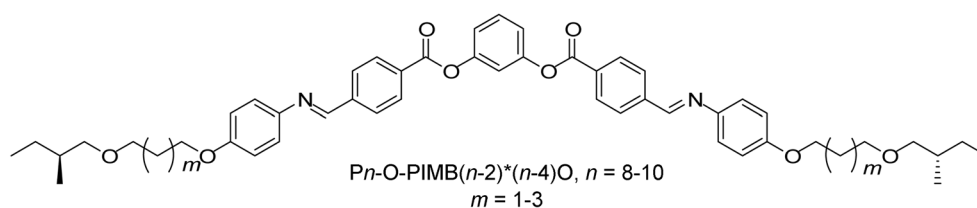
Figure 1 shows the diagram of mesomorphic transition temperatures for N(1,6)-*n*-O-PIMB(*n*-2)*-(*n*-4)O series and *Pn*-O-PIMB(*n*-2)*-(*n*-4)O series (in the inset) on cooling at a rate of 10 °C min⁻¹. The temperature ranges of the B2 phase in N(1,6)-*n*-O-PIMB(*n*-2)*-(*n*-4)O carrying the central naphthalene core were broader than that of the *Pn*-O-PIMB(*n*-2)*-(*n*-4)O with the central 1,3-phenylene core partly because of the steric and packing effect of intermolecular interaction. More detailed description of the mesomorphic behavior of each member of N(1,6)-*n*-O-PIMB(*n*-2)*-(*n*-4)O series will be given below.

The bent-shaped mesogen N(1,6)-8-O-PIMB6*-4O enantiotropically showed the B2 phase. On cooling from the isotropic liquid phase to the B2 phase, randomly oriented domains appeared. By applying a rectangular wave electric


Figure 1. Phase diagram of the N(1,6)-*n*-O-PIMB(*n*-2)*-(*n*-4)O series and *Pn*-O-PIMB(*n*-2)*-(*n*-4)O series (in the inset) on cooling.

field, the fan-shaped domains were developed to a relatively large size of smooth domains with an extinction direction parallel to the polarizer. However, the texture in the absence of an electric field showed the unusual switching behavior unlike the standard bent-shaped mesogens.^{29,30} Photomicrographs shown in Figure 2 display the switching behavior by applying a rectangular wave electric field. On field-off state, the texture remained unchanged except for a slight birefringence color change for 2-3 seconds as shown in Figure 2(a). This feature looks like bistable switching between two SmC_AP_F* states with opposite polarizations and racemic layer structures. However, this texture changes to the stripe domains of SmC_SP_A* immediately as shown in Figure 2(b), meaning that this is a field-induced change from the racemic SmC_SP_A* to the SmC_AP_F* state. Hence, the ground state is antiferroelectric (SmC_SP_A*) although it seems to be unstable.

The antiferroelectric phase (SmC_SP_A*) of ground state was more clearly assigned from switching current behavior on applying a triangular wave electric field and electric field dependence of the SHG measurement. The switching current behavior on applying a triangular wave electric field revealed two switching current peaks in a half cycle as shown in Figure 3(a), which means that this phase exhibits the antiferroelectricity. But two peaks are indistinct because of unstable ground state as shown in microscope texture observation. Figure 4 shows the applied field dependence of the SHG intensity. With decreasing the field, the system becomes SHG inactive and clear hysteresis behavior is observed. This hysteresis curve indicates the field-induced antiferroelectric-ferroelectric phase transition. Thus, we


Scheme 2

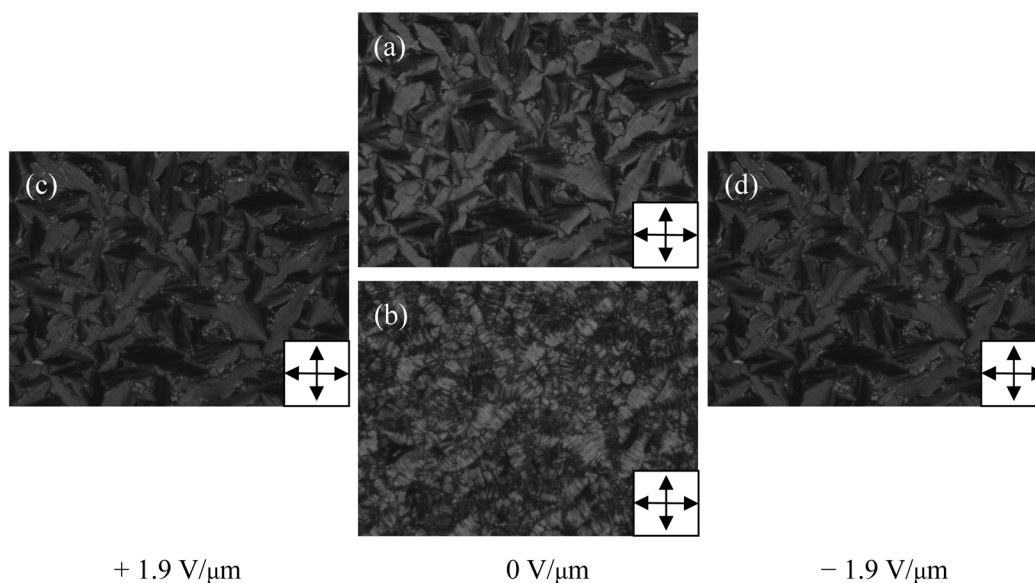


Figure 2. Photomicrographs of the switching behavior in the B2 phase in a $5.3 \mu\text{m}$ thick N(1,6)-8-O-PIMB6*-4O cell at 130°C . Circular domains of SmC_5P_A^* ($E = 0 \text{ V } \mu\text{m}^{-1}$) switch to SmC_AP_F^* under $E = \pm 1.9 \text{ V } \mu\text{m}^{-1}$ (c, d) under the application of an electric field, but (a) texture remained unchanged except for a slight birefringence color change after terminating the electric field for 2-3 seconds, then (b) the texture changes to the circular domains of SmC_5P_A^* . The polarizer and analyzer axes are along the edges of the photos.

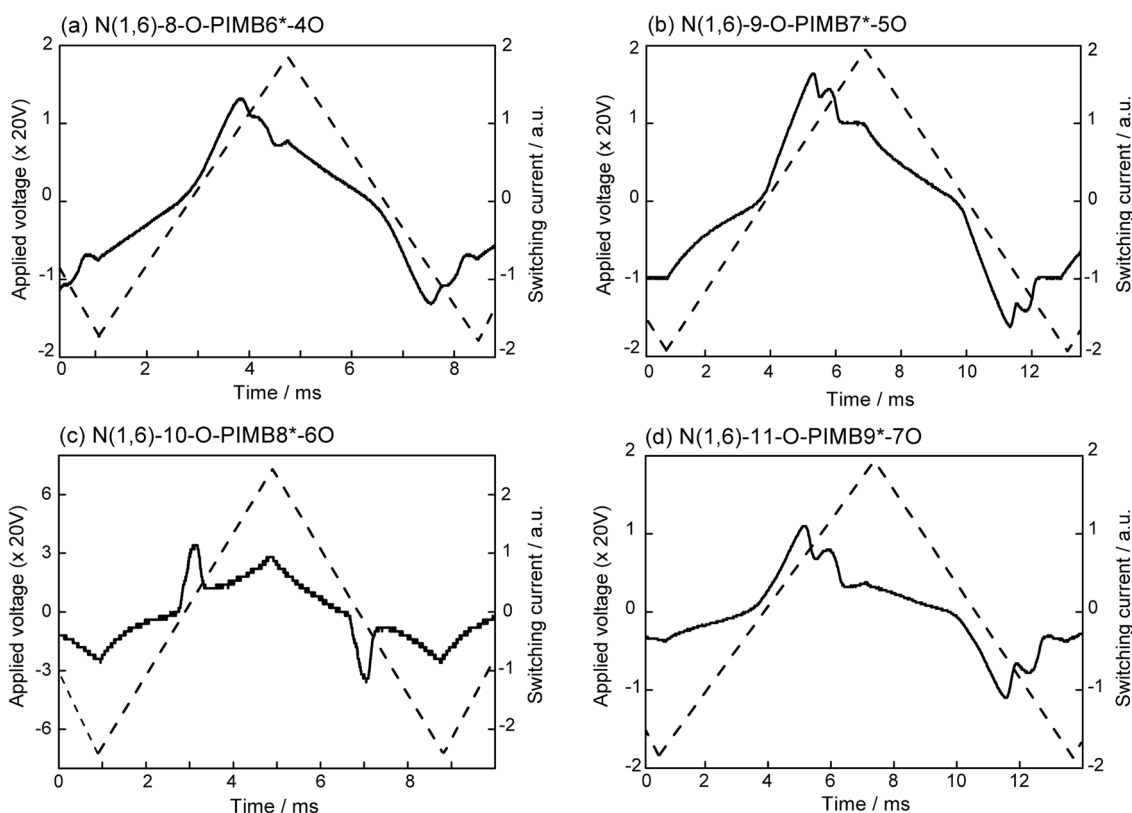


Figure 3. The polarization reversal current in the B2 phase: (a) N(1,6)-8-O-PIMB6*-4O at 130°C under the application of 66 V_{PP} triangular wave of 13.5 Hz , (b) N(1,6)-9-O-PIMB7*-5O at 140°C under the application of 80 V_{PP} triangular wave of 8.2 Hz , (c) N(1,6)-10-O-PIMB8*-6O at 140°C under the application of $260 \text{ V}_{\text{PP}}$ triangular wave of 12.8 Hz , (d) N(1,6)-11-O-PIMB9*-7O at 130°C under the application of 72 V_{PP} triangular wave of 8.7 Hz .

conclude that the stable state of N(1,6)-8-O-PIMB6*-4O is antiferroelectric (SmC_5P_A^*) as suggested by the texture and switching measurements.

The compounds N(1,6)-9-O-PIMB7*-5O and N(1,6)-11-O-PIMB9*-7O also enantiotropically exhibited the B2 phase. On cooling from the isotropic phase to the B2 phase,

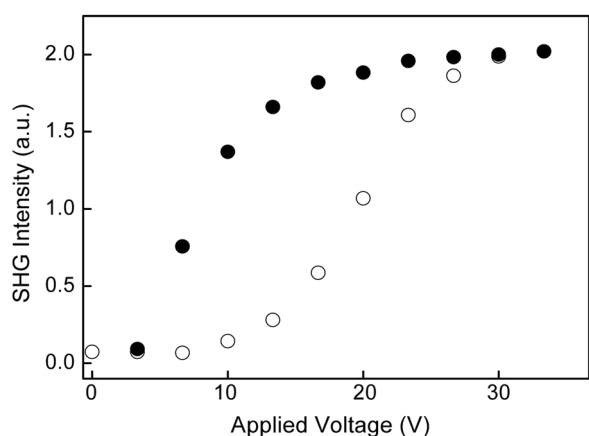


Figure 4. Electric field dependence of SHG intensity in a 5.3 μm thick cell of N(1,6)-8-O-PIMB6*-4O. A hysteresis curve was observed, indicating the field-induced antiferroelectric to ferroelectric phase transition. Open and closed circles stand for the data taken with increasing and decreasing voltage respectively.

randomly oriented domains were formed. These compounds exhibited fringe textures characteristic of typical SmC_sP_A^* in the absence of an electric field as shown in Figure 5. By applying a rectangular wave electric field, the fringes disappear and violet and green domains of relatively large size with an extinction direction parallel to the layer normal were observed, respectively, whereas characteristic striped domains appeared in the absence of an electric field. This texture change is the typical B2 phase observed in the standard bent-shaped mesogens and field-induced change from the SmC_sP_A^* to the SmC_AP_F^* in the racemic state. On applying a triangular wave electric field, two switching current peaks were observed in a half cycle as shown in Figure 3(b) and 3(d), respectively, which means that these materials exhibit antiferroelectricity (SmC_sP_A^*) in the stable state. However, the second peak was little smaller than the first one in N(1,6)-9-O-PIMB7*-5O (80 V_{pp} , 8.2 Hz, 140 $^\circ\text{C}$) and N(1,6)-11-O-PIMB9*-7O (72 V_{pp} , 8.7 Hz, 130 $^\circ\text{C}$). At the first switching peak, most of the domains in the cell

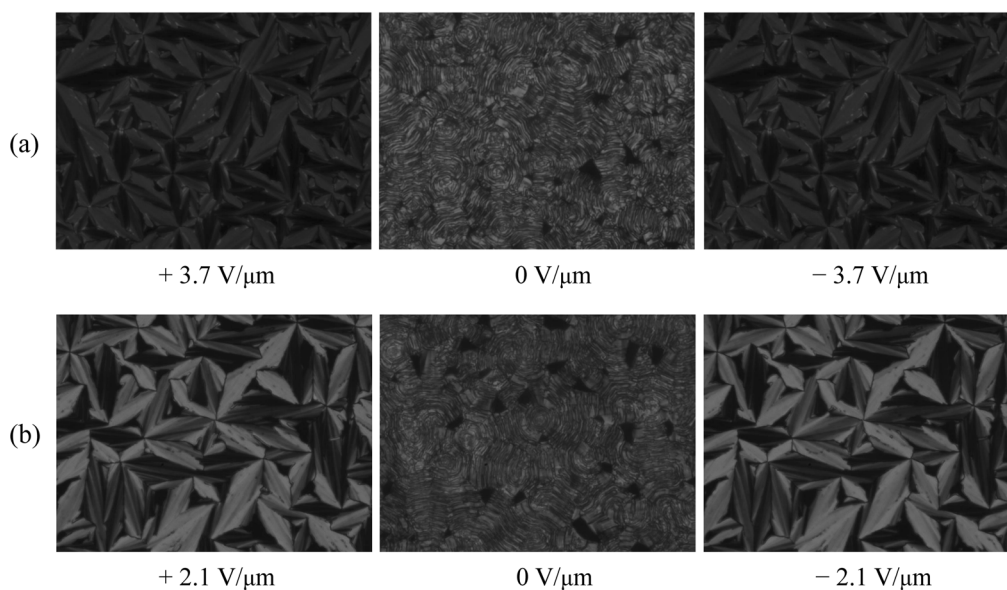


Figure 5. Photomicrographs of the switching behavior in the B2 phase: (a) 5.3 μm thick cell of N(1,6)-9-O-PIMB7*-5O at 140 $^\circ\text{C}$, (b) 9.4 μm thick cell of N(1,6)-11-O-PIMB9*-7O at 130 $^\circ\text{C}$. Circular domains of SmC_sP_A^* ($E = 0 \text{ V } \mu\text{m}^{-1}$) switch to SmC_AP_F^* under the application of an electric field.

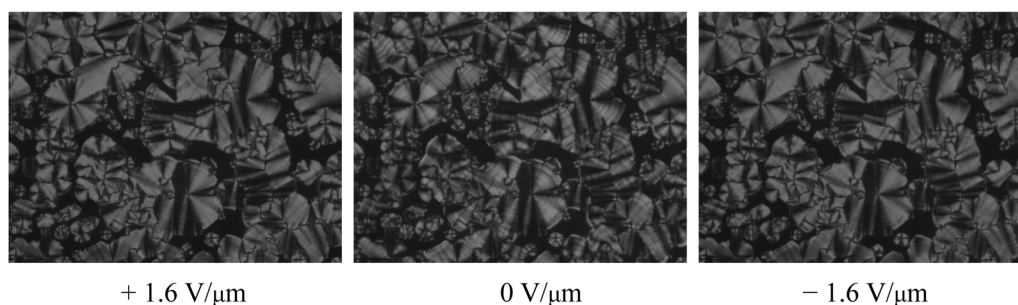


Figure 6. Photomicrographs showing the switching behavior in the B2 phase in a 6.2 μm thick cell of N(1,6)-10-O-PIMB8*-6O at 130 $^\circ\text{C}$. SmC_AP_F^* ($E = 0 \text{ V } \mu\text{m}^{-1}$) switches to SmC_AP_F^* under $E = \pm 1.6 \text{ V } \mu\text{m}^{-1}$ under the application of an electric field with a slight change of birefringence color.

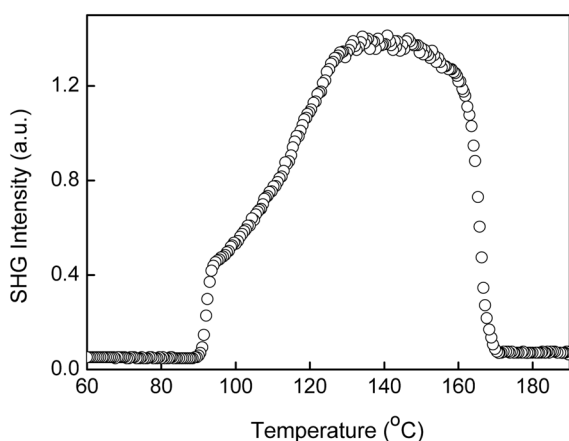


Figure 7. Temperature dependence of the SHG intensity in N(1,6)-10-O-PIMB8*-6O.

change from ferroelectric to ferroelectric and the rest of them from ferroelectric to antiferroelectric. At the second switching peak, a relatively small fraction of the antiferroelectric domains switch to ferroelectric. This untypical antiferroelectric switching current response feature was also observed in Pn -O-PIMB($n-2$)*-($n-4$)O series in our previous study.²⁶ However, it is not clear why these compounds which have chiral terminal chain prepared from (*S*)-(-)-2-methyl-1-butanol show these phenomena.

The compound N(1,6)-10-O-PIMB8*-6O showed quite different electro-optical switching behavior as shown in Figure 6. In these photomicrographs, we observed smooth domains that have extinctions parallel to the layer normal under an electric field. The texture remained unchanged except for a slight birefringence color change after terminating the electric field. This feature indicates bistable switching between two $SmC_A P_F^*$ states with opposite polarizations and racemic layer structure. A single switching current peak in the polarization switching current measurement was revealed in a half cycle on applying a triangular wave voltage as shown in Figure 3(c), which indicates ferroelectricity. Figure 7 shows the SHG intensity as a function of temperature in the absence of an electric field of N(1,6)-10-O-PIMB8*-6O. The SHG activity without an electric field indicates the polar order. On cooling from the isotropic liquid phase, an onset of SHG intensity was observed at the transition temperature to the B2 phase and the SHG intensity increases with decreasing temperature. On further cooling the SHG intensity begins to decrease until it becomes inactive at about 85 °C. This result leads to the conclusion that N(1,6)-10-O-PIMB8*-6O clearly exhibits a ferroelectric state ($SmC_A P_F^*$) in nature based on the texture and polarization switching current measurements.

Discussion

Provided that the systems keep the racemic layer structure, the difference between the ferroelectric and antiferroelectric ordering in bent-shaped molecules exist in the tilting direction between adjacent smectic layers caused by the

effect of interlayer interaction. Particularly, the terminal chain in bent-shaped molecules plays an important role in determining of the particular phase structures. This property is very strictly established, if the parking of the central cores is tight like in bent-shaped mesogens. Actually, recently Kumazawa *et al.*²⁵ and Lee *et al.*²⁶ reported the odd-even behavior for the emergence of ferroelectricity and antiferroelectricity depending on the number of carbons and the position of the chiral carbon along the terminal chains in two homologous series of bent-shaped molecules, Pn -O-PIMB($n-2$)* and their oxygen analogues Pn -O-PIMB($n-2$)*-($n-4$)O; The compounds exhibit antiferroelectric the $SmC_S P_A^*$ phase when n is odd, whereas they exhibit the ferroelectric $SmC_A P_F^*$ phase when n is even. Moreover, Nishida *et al.*³¹ developed a theoretical formula including the interlayer steric interaction, dipole-dipole interaction and van der Waals attraction to explain the polar order and tilt order between adjacent layers. However, these two homologous series are normally symmetric and the closed packing of symmetrical resorcinol central bent core makes the position of end of the terminal chains fixed. Namely, the chiral carbon is always located at the same position from the end of the terminal chains, and then the directions of the methyl groups connected to the chiral centers can be fixed.

However, as mentioned above, N(1,6)- n -O-PIMB($n-2$)*-($n-4$)O where the side wings are asymmetrically substituted to the central core based on 1,6-dihydroxynaphthalene did not perfectly follow the odd-even behavior although the terminal alkyl chain is the same in previous compounds Pn -O-PIMB($n-2$)*-($n-4$)O.²⁶ The polar structures of the newly synthesized N(1,6)- n -O-PIMB($n-2$)*-($n-4$)O are summarized in Table 2.

The antiferroelectric phase is always brought about from N(1,6)- n -O-PIMB($n-2$)*-($n-4$)O, when n is odd and the position of the chiral center from the phenoxy oxygen in the terminal group is also odd. This result is identical with Pn -O-PIMB($n-2$)*-($n-4$)O series.²⁶ However, when n is even, N(1,6)-10-O-PIMB8*-6O exhibits the ferroelectric phase but N(1,6)-8-O-PIMB6*-4O exhibits the antiferroelectric phase. That is to say, the compound with a longer terminal chain follows the nature of odd-even behavior as expected, but the compound with a relatively shorter terminal chain disregards for odd-even rule. The same rule has also been observed in the compounds with asymmetrical resorcinol central bent core having terminal chains of different lengths.²⁷ In the present compounds, the same situation arises from the asymmetric side wings due to the asymmetrical naphthalene central core. In other words, the asymmetrical central core

Table 2. Polar structures of the B2 phase in N(1,6)- n -O-PIMB($n-2$)*-($n-4$)O series

compound	polar structure	polar order
N(1,6)-8-O-PIMB6*-4O	$SmC_S P_A^*$	antiferroelectric
N(1,6)-9-O-PIMB7*-5O	$SmC_S P_A^*$	antiferroelectric
N(1,6)-10-O-PIMB8*-6O	$SmC_A P_F^*$	ferroelectric
N(1,6)-11-O-PIMB9*-7O	$SmC_S P_A^*$	antiferroelectric

decreases the closed packing efficiency within a layer. The closed packing means that the bent cores are tightly fixed, so that the shift of cores along the layer normal is strongly prohibited. Consequently, the lack of uniform interlayer interaction results between adjacent layers, which were caused by the asymmetrical naphthalene central core. Thus, we can suppose that the relatively weak closed packing caused by asymmetrical central core varied the position of the terminal carbon and then generates the exception of odd-even rule in N(1,6)-*n*-O-PIMB(*n*-2)*-(*n*-4)O series.

In the previous subsection, we explained unique feature that N(1,6)-8-O-PIMB6*-4O, where *n* is even, exhibited the ferroelectric (SmC_AP_F*) feature for a few seconds on field-off state although the ground state showed unstable anti-ferroelectric (SmC_SP_A*) phase. This interesting phenomenon may come from the competition between the effect of central core and terminal chain for generating the more stable polar order. In other words, although this compound has the potentiality of ferroelectric polar order according to the terminal chain of even, the loosening packing caused by asymmetrical central core prefers the antiferroelectric polar order in the most stable state. On the contrary, in the case of N(1,6)-10-O-PIMB8*-6O, the effect of longer terminal chain is bigger than the central core and then ferroelectric phase appears in stable state. Thus, these results clearly show that the emergence of particular polar order of the SmCP phase depends on the structure of central core and the terminal chain length. We are synthesizing N(1,6)-*n*-O-PIMB(*n*-2)*-(*n*-4)O (*n* = 12 and 13) to confirm the odd-even effect in this homologue. The results will be presented in the near future.

Conclusion

We have synthesized new chiral bent-shaped liquid crystals, N(1,6)-*n*-O-PIMB(*n*-2)*-(*n*-4)O (*n* = 8-11), and studied phase behaviors in order to confirm the effect of the molecular structure on the emergence of polar ordering in phase structure. Odd *n* (*n* = 9 and 11) compounds, N(1,6)-9-O-PIMB7*-5O and N(1,6)-11-O-PIMB9*-7O always exhibit antiferroelectric phase, whereas even *n* (*n* = 8 and 10) compounds follow a more flexible rule: N(1,6)-10-O-PIMB8*-6O exhibits the ferroelectric phase but N(1,6)-8-O-PIMB6*-4O exhibits the antiferroelectric phase. These results indicate that the polar order strongly depends on the symmetry of molecules. Namely, due to the asymmetrical naphthalene central core, the closed packing within each layer decreases and then the influence of interlayer steric interaction of chiral terminal chain also decreases. Thus, it is obvious that the emergence of ferroelectricity and antiferroelectricity must be caused by both the structure of central core and terminal chain.

References

1. Mayer, R. B.; Liebert, L.; Strzelecki, L.; Keller, P. *J. Phys. (Fr)*

- Lett.* **1975**, *36*, L69.
2. Chandani, A. D. L.; Gorecka, E.; Ouchi, Y.; Takezoe, H.; Hukuda, A. *Jpn. J. Appl. Phys.* **1989**, *28*, L1265.
3. Niori, T.; Sekine, T.; Watanabe, J.; Furukawa, T.; Takezoe, H. *J. Mater. Chem.* **1996**, *6*, 1231.
4. Takezoe, H.; Takanishi, Y. *Jpn. J. Appl. Phys.* **2006**, *45*, 597.
5. Pelzl, G.; Schroeder, M.; Dunemann, U.; Diele, S.; Weissflog, W.; Jones, C.; Colemann, D.; Clack, N.; Stannarius, R.; Li, J.; Das, B.; Grande, S. *J. Mater. Chem.* **2004**, *14*, 2492.
6. Nakata, M.; Link, D. R.; Thisayukta, J.; Takanishi, Y.; Ishikawa, K.; Watanabe, J.; Takezoe, H. *J. Mater. Chem.* **2001**, *11*, 2694.
7. Niwano, H.; Nakata, M.; Thisayukta, J.; Link, D. R.; Takezoe, H.; Watanabe, J. *J. Am. Chem. Soc.* **2004**, *108*, 14889.
8. Thisayukta, J.; Niwano, H.; Takezoe, H.; Watanabe, J. *J. Am. Chem. Soc.* **2002**, *124*, 3354.
9. Thisayukta, J.; Niwano, H.; Takezoe, H.; Watanabe, J. *J. Mater. Chem.* **2001**, *11*, 2717.
10. Nakata, M.; Link, D. R.; Araoka, F.; Thisayukta, J.; Takanishi, Y.; Ishikawa, K.; Watanabe, J.; Takezoe, H. *Liq. Cryst.* **2001**, *28*, 1301.
11. Nakata, M.; Link, D. R.; Takanishi, Y.; Takahashi, Y.; Thisayukta, J.; Niwano, H.; Coleman, D. A.; Watanabe, J.; Lida, A.; Clark, N. A.; Takezoe, H. *Phys. Rev. E* **2005**, *71*, 011705.
12. Lee, S. K.; Park, C. W.; Lee, J. G.; Kang, K.-T.; Nishida, K.; Shimbo, Y.; Takanishi, Y.; Takezoe, H. *Liq. Cryst.* **2005**, *32*, 1205.
13. Link, D. R.; Natale, G.; Shao, R.; MacLennan, J. E.; Clark, N. A.; Körblová, E.; Walba, D. M. *Science* **1997**, *278*, 1924.
14. Walba, D. M.; Körblová, E.; Shao, R.; MacLennan, J. E.; Link, D. R.; Glaser, M. A.; Clark, N. A. *Science* **2000**, *288*, 2181.
15. Niori, T.; Yamamoto, J.; Yokoyama, H. *Mol. Cryst. Liq. Cryst.* **2004**, *411*, 1325.
16. Olson, D. A.; Veun, M.; Cady, A.; D'agostino, M. V.; Johnson, P. M.; Nguyen, H. T.; Chen, L. C.; Huang, C. C. *Phys. Rev. E* **2001**, *63*, 041702.
17. Keith, C.; Reddy, R. A.; Hahn, H.; Lang, H.; Schierske, C. *Chem. Commun.* **2004**, *25*, 1898.
18. Dantgraber, G.; Eremin, A.; Diele, S.; Hauser, A.; Kresse, H.; Pelzl, G.; Tschierske, C. *Angew. Chem., Int. Ed.* **2002**, *41*, 2408.
19. Nadasi, H.; Weissflog, W.; Eremin, A.; Pelzl, G.; Diele, S.; Das, B.; Grande, S. *J. Mater. Chem.* **2002**, *12*, 1316.
20. Bedel, J. P.; Rouillon, J. C.; Maroerou, J. P.; Lauerre, M.; Nguyen, H. T.; Achard, M. F. *Liq. Cryst.* **2000**, *27*, 103.
21. Bedel, J. P.; Rouillon, J. C.; Maroerou, J. P.; Lauerre, M.; Nguyen, H. T.; Achard, M. F. *Liq. Cryst.* **2001**, *28*, 1285.
22. Reddy, R. A.; Sadashiva, B. K. *J. Mater. Chem.* **2002**, *12*, 2627.
23. Reddy, R. A.; Schroder, M. W.; Boddyagin, M.; Kresse, H.; Diele, S.; Pezel, G.; Weissflog, W. *Angew. Chem., Int. Ed.* **2005**, *44*, 774.
24. Reddy, R. A.; Sadashiva, B. K. *J. Mater. Chem.* **2004**, *14*, 1936.
25. Kumazawa, K.; Nakada, M.; Araoka, F.; Takanishi, Y.; Ishikawa, K.; Watanabe, J.; Takezoe, H. *J. Mater. Chem.* **2004**, *14*, 157.
26. Lee, S. K.; Heo, S.; Lee, J. G.; Kang, K.-T.; Kumazawa, K.; Nishida, K.; Shimbo, Y.; Takanishi, Y.; Watanabe, J.; Doi, T.; Takahashi, T.; Takezoe, H. *J. Am. Chem. Soc.* **2005**, *127*, 11085.
27. Nishida, K.; Kim, W. J.; Lee, S. K.; Heo, S.; Lee, J. G.; Kang, K.-T.; Takanishi, Y.; Ishikawa, K.; Watanabe, J.; Takezoe, H. *Jpn. J. Appl. Phys.* **2006**, *45*, L329.
28. Lee, S. K.; Naito, Y.; Shi, L.; Tokita, M.; Takezoe, H.; Watanabe, J. *Liq. Cryst.* **2007**, *34*, 935.
29. Zennyoji, M.; Takanishi, Y.; Ishikawa, K.; Thisayukta, J.; Watanabe, J.; Takezoe, H. *J. Mater. Chem.* **1999**, *9*, 2775.
30. Zennyoji, M.; Takanishi, Y.; Ishikawa, K.; Thisayukta, J.; Watanabe, J.; Takezoe, H. *Jpn. J. Appl. Phys.* **2000**, *39*, 3536.
31. Nishida, K.; Cepic, M.; Kim, W. J.; Lee, S. K.; Heo, S.; Lee, J. G.; Takanishi, Y.; Ishikawa, K.; Kang, K.-T.; Watanabe, J.; Takezoe, H. *Phys. Rev. E* **2006**, *74*, 021704.